

# Chemistry A European Journal

 **Chemistry  
Europe**  
European Chemical  
Societies Publishing

## Accepted Article

**Title:** DNA Adduct Detection after Post-Labeling Technique with PCR Amplification (DNA-ADAPT-qPCR) Identifies the Pre-Ribosomal RNA Gene as a Direct Target of Platinum–Acridine Anticancer Agents

**Authors:** Xiyuan Yao and Ulrich Bierbach

This manuscript has been accepted after peer review and appears as an Accepted Article online prior to editing, proofing, and formal publication of the final Version of Record (VoR). This work is currently citable by using the Digital Object Identifier (DOI) given below. The VoR will be published online in Early View as soon as possible and may be different to this Accepted Article as a result of editing. Readers should obtain the VoR from the journal website shown below when it is published to ensure accuracy of information. The authors are responsible for the content of this Accepted Article.

**To be cited as:** *Chem. Eur. J.* 10.1002/chem.202102263

**Link to VoR:** <https://doi.org/10.1002/chem.202102263>

WILEY-VCH

**DNA Adduct Detection after Post-Labeling Technique with PCR Amplification (DNA-ADAPT-qPCR) Identifies the Pre-Ribosomal RNA Gene as a Direct Target of Platinum-Acridine Anticancer Agents**

Xiyuan Yao and Ulrich Bierbach\*

*Dr. X. Yao, Prof. U. Bierbach*

*Department of Chemistry*

*Wake Forest University*

*Wake Downtown Campus*

*455 Vine St.*

*Winston-Salem, NC 27101 (USA)*

*E-mail: bierbau@wfu.edu*

Accepted Manuscript

**Abstract:**

To study the DNA damage caused by a potent platinum–acridine anticancer agent (PA) in cancer cells, an assay based on biorthogonal post-labeling using a click chemistry-enabled, azide-modified derivative (APA) was developed. The method involves biotinylation, affinity capture, and bead-based enrichment of APA-modified genomic DNA. The key steps of the assay were validated and optimized in model duplexes, including full-length plasmids, restriction fragments, and a DNA ladder. Native DNA treated with APA and subsequently subjected to post-labeling with a biotin affinity tag was enzymatically digested and fragments were analyzed by in-line LC-MS and MS/MS. The monofunctional–intercalative adducts formed by APA in 5'-pyrimidine/guanine sequences in double-stranded DNA are quantitatively biotinylated by strain-promoted 1,3-dipolar cycloaddition chemistry. When applied to DNA extracted from A549 lung cancer cells, the assay in combination with qPCR amplification demonstrates that platinum–acridines form adducts in the gene sequences encoding pre-ribosomal RNA, a potential pharmacological target of these agents.

## Introduction

Cytochemical and immunocytochemical imaging and affinity pulldown techniques have become indispensable tools for studying the cellular mechanism of DNA-targeted small molecules,<sup>[1]</sup> including platinum-based anticancer agents.<sup>[2]</sup> Fluorescent post-labeling using bioorthogonal click chemistry has also been instrumental for probing the subcellular distribution of platinum–acridine hybrid agents, a novel class of highly potent cytotoxics.<sup>[3]</sup> The most potent derivatives of this class, such as PA (Figure 1A), show a unique anticancer spectrum and promising preclinical potential.<sup>[4]</sup> The unique monofunctional–intercalative DNA adducts formed by platinum–acridines induce replication fork arrest, which leads to DNA double-strand breaks,<sup>[5]</sup> and inhibit RNA polymerase II (Pol II)-mediated transcription.<sup>[6]</sup> Data from structure–activity and mechanistic studies in mammalian cells and chemical genomics screening in yeast are consistent with the hypothesis that DNA is the pharmacological target of these agents.<sup>[7]</sup>

Most strikingly, using fluorescent post-labeling of click chemistry-enabled derivatives, we demonstrated that platinum–acridines accumulate in the nucleoli in cells in interphase at significantly higher levels than in the surrounding chromatin.<sup>[3b]</sup> Because the nucleolus is the site of precursor ribosomal RNA (pre-rRNA) synthesis, which is a critical step in ribosome biogenesis, the pre-rRNA gene repeats (“rDNA”) transcribed by RNA polymerase I (Pol I) are a promising target for DNA-directed chemotherapies.<sup>[8]</sup> Lung cancer cells in interphase treated with platinum–acridines showed a distinct time-dependent shrinkage of the nucleoli and a concomitant quenching of pre-rRNA synthesis.<sup>[3a]</sup> Immunocytochemical staining of the nuclei in treated lung cancer cells using a phosphorylated histone 2A-directed antibody (anti- $\gamma$ -H2AX) provided additional circumstantial evidence that platinum–acridines may damage nucleolar rDNA.<sup>[5a]</sup> In these experiments DNA double-strand breaks were detected in the regions surrounding the nucleoli

(nucleolar caps), which are the sites of rDNA repair.<sup>[9]</sup> Based on these observations we hypothesized that the high level of PA in the nucleoli might render rDNA a *direct* target of these agents. However, neither of the above techniques provided insight into the ultimate cause of the observed cellular responses and whether permanent Pt–rDNA adducts may be involved in the mechanism triggering apoptotic cancer cell death.

In the present study, we employed a terminal azide-functionalized derivative of PA, APA (Figure 1A), to detect Pt–rDNA adducts in cancer cells using chemical labeling and affinity capture. We designed an assay based on biotin post-labeling of covalent, azide-containing DNA adducts of APA, which we termed *DNA Adduct Detection after Post-labeling Technique (DNA-ADAPT)* (Figure 1B). The bioorthogonal chemistry of DNA adduct labeling was validated by bottom-up digestion of APA-modified native DNA in conjunction with MS/MS fragmentation, and the pull-down was tested and optimized with plasmid DNA and oligodeoxyribonucleotides. Finally, we applied the technique in combination with quantitative PCR (DNA-ADAPT–qPCR) to APA-modified DNA isolated from treated cancer cells to demonstrate that the 47S pre-rRNA gene is indeed targeted by platinum–acridines.

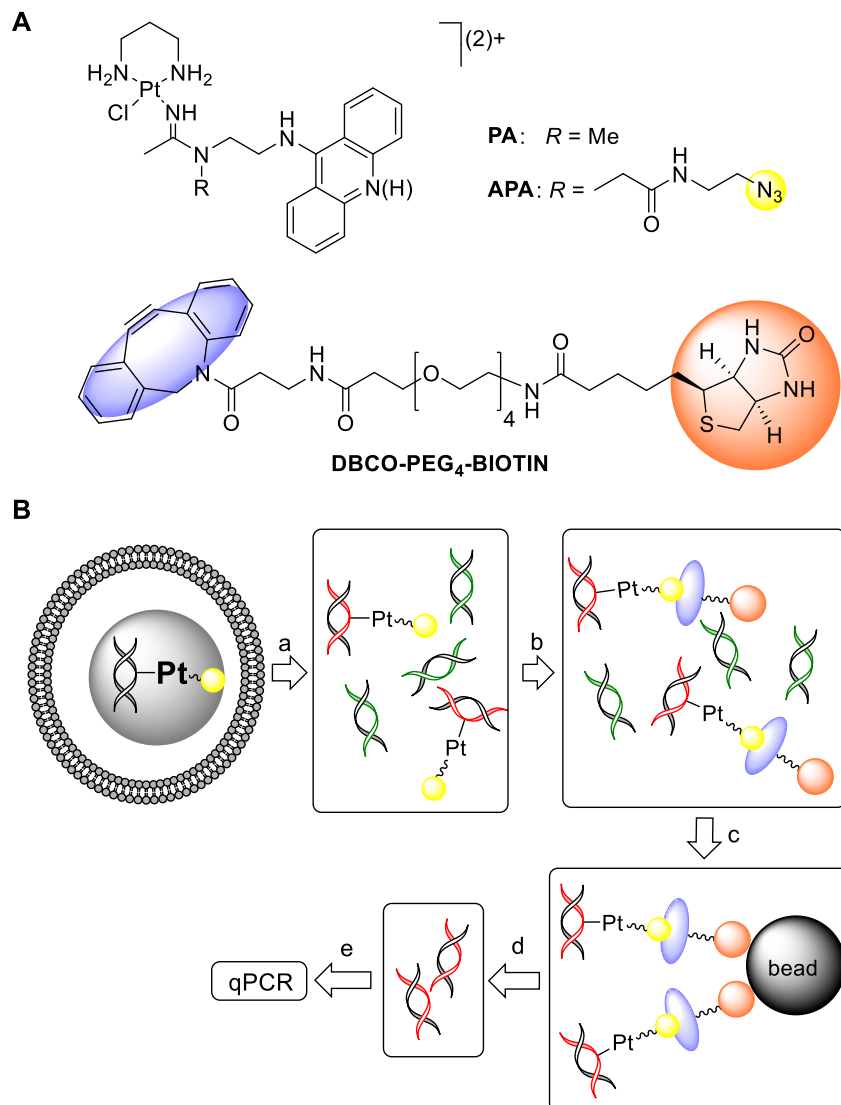


**Figure 1.** Using an azide-functionalized platinum–acridine derivative (APA) to affinity-capture and detect Pt-modified genomic DNA. (A) Chemical structures of compound APA and the biotin affinity tag, DBCO-PEG<sub>4</sub>-BIOTIN; the nitrate counter ions for PA and APA are not shown. (B) Workflow of DNA-ADAPT: (a) Extraction of genomic DNA from cancer cells treated with APA, purification, fragmentation; (b) post-labeling of Pt-containing fragments with DBCO-PEG<sub>4</sub>-BIOTIN; (c) affinity capture on streptavidin-coated magnetic beads; (d) release of enriched target DNA sequences from the beads; (e) analysis of DNA by quantitative PCR (qPCR). For details, see the text and Experimental Section.

## Results and Discussion

### Design of DNA-ADAPT

To detect potential rDNA damage by APA, a chemically robust and sensitive technique is required to capture and enrich Pt–rDNA adducts. APA was derived from compound PA by replacing the methyl group (*R*) on the amino nitrogen of amidine with a *N*-(2-azidoethyl)propionamide group (Figure 1A; see the SI for synthetic details). This modification has previously been demonstrated to not interfere with the DNA binding of platinum–acridine agents and their subcellular localization.<sup>[3b, 7a]</sup> The level of APA detected in DNA extracted from A549 cells (5 drug molecules per 10,000 base pairs when treated at 10  $\mu$ M APA for 6 hours) was similar to that determined for unmodified platinum–acridines.<sup>[5b, 10]</sup> Likewise, APA and the parent compound produce a similar cytotoxic response in this cell line ( $49 \pm 8$  nM vs.  $29 \pm 3$  nM for PA<sup>[4a]</sup>), suggesting that APA mimics PA biologically.

The overall strategy of the assay is outlined in Figure 1B. Cancer cells are treated with APA under conditions that do not compromise cell viability while producing the desired level of Pt–DNA adducts. DNA is extracted from the cells and purified to remove protein and RNA, resulting in a fraction of Pt-modified and unmodified DNA, which is subjected to sonication to produce qPCR-compatible, 100–500 base-pair fragments of double-stranded DNA (dsDNA). DBCO-PEG<sub>4</sub>-BIOTIN (Figure 1A) is then introduced to post-label the Pt-modified DNA fragments with a biotin affinity tag via strain-promoted click chemistry. Biotin-labeled Pt–DNA is affinity purified using streptavidin-coated magnetic beads. After removal of unlabeled DNA, the platinated–biotinylated DNA is dissociated from the beads by incubation with sodium cyanide under conditions that completely reverse the monofunctional adducts.<sup>[11]</sup> The enriched, affinity-

purified DNA is subjected to a clean-up step, ultrasonically sheared, and subsequently analyzed by quantitative PCR (qPCR) to detect potential target sequences (DNA-ADAPT-qPCR).

### Validation of key reactions

To test the chemical feasibility of ADAPT in dsDNA, the two key reactions, (i) monofunctional adduct formation, which involves platination of guanine (G)-N7 in the major groove of the duplex,<sup>[5b]</sup> and (ii) labeling of adducts using copper-free click chemistry, were studied at atomic resolution in native DNA (Figure 2A). After reaction of calf thymus DNA with APA, samples were enzymatically digested to afford a pool of Pt-modified and unmodified oligodeoxyribonucleotides and 2'-deoxyribonucleosides (Figure 2A). In a parallel experiment, the APA-modified DNA was treated with DBCO-PEG<sub>4</sub>-BIOTIN to biotinylate the adducts prior to endonucleolytic digestion (Figure 2A). The resulting mixtures were then separated by reverse-phase HPLC (Figure 2B) and analyzed by electrospray mass spectrometry (ESMS). Target ions were further subjected to MS/MS fragmentation to confirm the nucleobase specificity and sequence context of adduct formation.

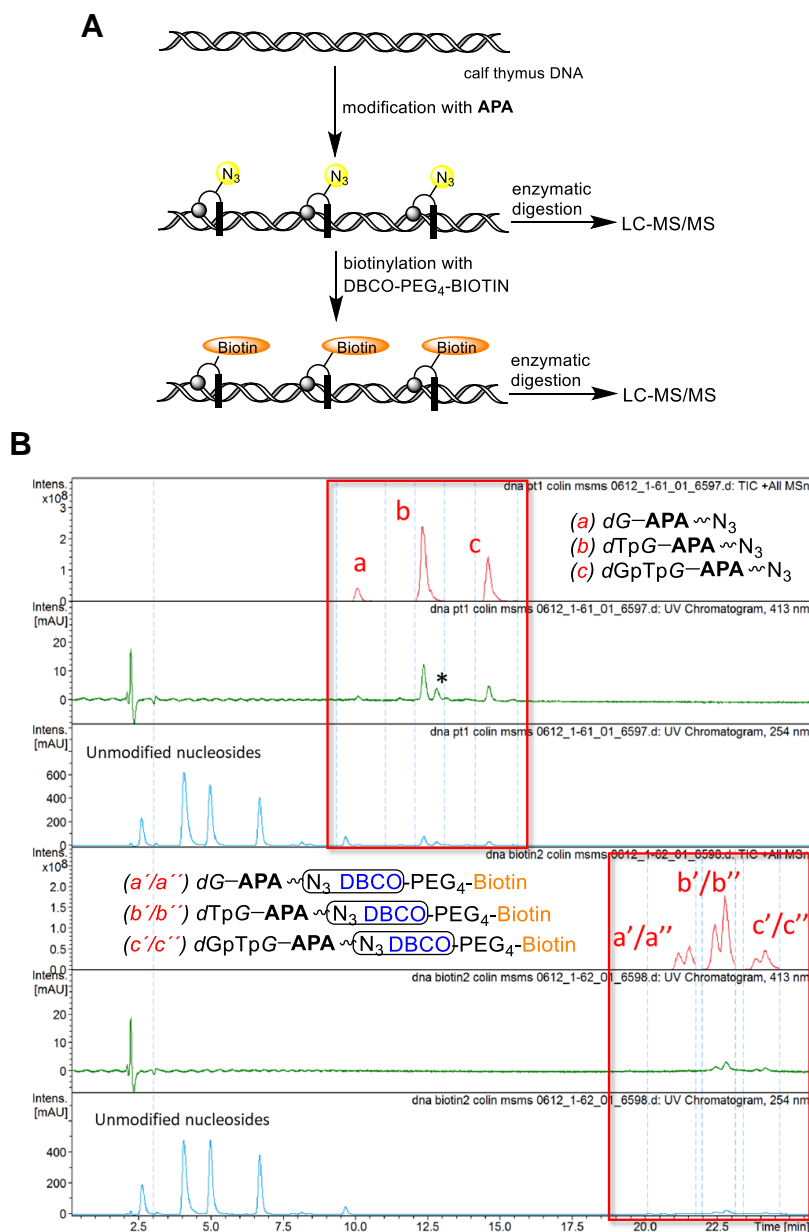


**Figure 2.** (A) Structural characterization of monofunctional–intercalative G-N7 adducts before and after post-labeling in native dsDNA. (B) Analysis of enzymatic digests: calf-thymus DNA was treated with APA and enzymatically digested before (top traces) or after post-labeling with DBCO-PEG<sub>4</sub>-BIOTIN (bottom traces) yielding mixtures of Pt-modified and unmodified deoxyribonucleos(t)ides, which were separated by reverse-phase HPLC. APA-modified fragments (fractions a, b, and c) and the corresponding biotinylated forms (fractions a'/a'', b'/b'', c'/c''),

and c'/c'') were identified in HPLC traces at a wavelength specific for the acridine chromophore (413 nm, green traces) and analyzed by ESMS. Selected ions were analyzed by MS/MS (see the SI for a detailed structural analysis of major adduct fragments). Red and blue traces are total ion count (TIC) chromatograms and UV chromatograms recorded at 254 nm, respectively. The asterisk denotes an unidentified product.

Enzymatic digestion resulted in the four native 2'-deoxyribonucleosides and three platinated fragments, dG\* (Pt-modified 2'-deoxyguanosine), 5'-TpG\*-3', and 5'-GpTpG\*-3' (asterisks indicate the sites of the Pt adducts) (Figure 2B). A similar digestion pattern is observed after treatment of the dsDNA with the DBCO-PEG<sub>4</sub>-BIOTIN tag (bottom three traces in Figure 2B) with the corresponding peaks shifted to longer retention times. The 1,3 dipolar cycloaddition between the terminal azide moiety in APA and DBCO yields the expected pairs of triazene regioisomers<sup>[3a]</sup> (labeled ' and '' in Figure 2B). Most importantly, the reaction of APA adducts in the DNA major groove with the DBCO affinity tag proved to be quantitative, which renders it a suitable, highly efficient post-labeling step for the proposed assay. Furthermore, the data confirms that introduction of a linker with a terminal azide group does not alter the well-established propensity of platinum–acridines to form adducts with G-N7 at 5'-pyrimidine/purine sites.<sup>[5b]</sup> This observation provides further support that APA faithfully mimics critical features of the parent PA.

### **Affinity purification of APA-modified, biotinylated DNA**

In addition to the post-labeling chemistry (biotinylation), the suitability of ADAPT for detecting Pt-modified genomic DNA critically depends on affinity pull-down of the nucleic acid and its purification using streptavidin magnetic beads. Initially, the feasibility of this step was tested using linearized plasmid DNA (Figure 3A). The plasmid pBR322 was modified with APA at a platinum-to-base pair ratio of 0.01 and then mixed with untreated pUC19 plasmid. After treatment with DBCO-PEG<sub>4</sub>-BIOTIN, samples were subjected to magnetic bead purification and analyzed by agarose gel electrophoresis (Figure 3B). The recovery of plasmid was estimated from the intensities of ethidium-stained bands containing affinity-purified DNA relative to a control that had not undergone bead purification. Approximately 8% of pBR322 could be recovered under these conditions whereas no pUC19 plasmid was detectable. This experiment demonstrates that ADAPT selectively enriches DNA modified with APA from a stoichiometric mixture of the two plasmids.

To better mimic sheared DNA, which will be used in the downstream qPCR amplification reactions, and to optimize the reaction conditions, we also performed the assay in restriction fragments 375 bp to 4361 bp in length generated from pBR322 plasmid. Doubling the amount of streptavidin-coated beads resulted in a modest increase in recovery of affinity-purified DNA from 10% to 14% (Figure S7). On the other hand, 10-fold DBCO-PEG<sub>4</sub>-BIOTIN in the mixtures completely abrogated affinity capture, consistent with excess biotinylation reagent blocking binding sites, which diminishes the binding capacity of the beads (Figure S9). Inefficient dissociation of DNA from the beads in the last step of the assay can be ruled out as a yield-limiting factor, as treatment of the beads with higher sodium cyanide concentrations for extended time periods did not result in higher DNA recoveries (Figure S8).

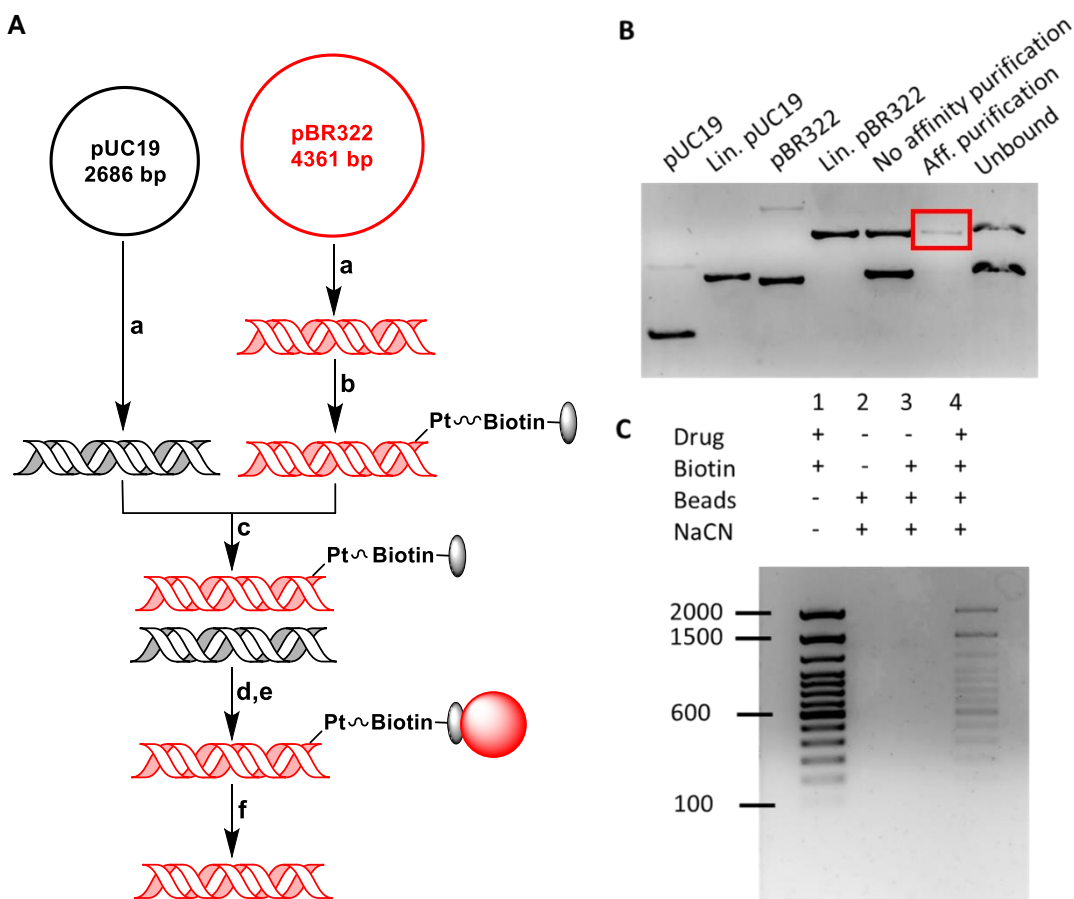


**Figure 3.** Validation and optimization of DNA purification by affinity capture in model duplexes.

(A) Assay design for plasmid DNA: (a) Preparation of linearized forms of two plasmids; (b) treatment of pBR322 with APA and post-labeling with DBCO-PEG<sub>4</sub>-BIOTIN (2 steps); (c) pooling of unmodified pUC19 and APA-modified pBR322 plasmid samples; (d) affinity capture on beads (red spheres) and (e) removal of nonspecifically bound plasmid; (f) dissociation of affinity-captured pBR322 and detection/quantification by gel electrophoresis. (B) Agarose gel for affinity purification of plasmid DNA. The recovered pBR322 (8%) is highlighted with a red box. (C) Agarose gel for affinity purification of a DNA ladder. The DNA was modified with APA at a drug-to-base pair ratio of 0.02. Lane assignments: 1-unpurified DNA, 2-unplatinated/unbiotinylated control, 3-unplatinated control, 4-ADAPT-purified DNA. The

estimated cumulative recovery of DNA (lane 4 vs. lane 1) is 11% (Image J software). (An accurate quantification was not possible because of variabilities in the ethidium staining efficiency for individual fragments.)

Using the optimized conditions, DNA-ADAPT was finally validated using a 100–2000-bp DNA ladder (Figure 3C). Visual inspection of the agarose gel confirms that sequences as short as 200 bp could be pulled down. The results show that the overall recovery of DNA duplexes based on integrated band intensities for all fragments is approximately 11% of the non-affinity purified control lane. For some sequences, the recoveries exceeded those observed with the (digested) plasmid DNA, resulting in 15% recovery for the 2000-bp, 20% for the 1500-bp, and 18% for the 600-bp fragment. Relatively weaker bands are observed for the shorter fragments in both treatment and control lanes, which may be due to inefficient staining of the DNA with ethidium bromide or indicate a lower abundance in the fragment mixture.

Post-labeling has previously been applied to platinum-based pharmacophores both in intact cells and cellular extracts.<sup>[2a, b, e]</sup> The method circumvents several limitations encountered if the bioactive molecule of interest is modified with an affinity label or a reporter group prior to treating cultured cells. These include altered uptake, subcellular distribution, and target interactions caused by the structural modification.<sup>[3a, 12]</sup> Nonspecific sequestration of biotinylated probes by endogenous biotin-binding proteins is another potential drawback<sup>[13]</sup> that can be overcome by labeling the probe after it has engaged with its cellular target. DNA-ADAPT combines exquisitely efficient biotinylation at the damage site with quantitative reversal of the Pt-mediated cross-links for purification of bead-captured APA-modified DNA.

### Application of DNA-ADAPT–qPCR to DNA extracted from cancer cells

Finally, we tested our hypothesis that platinum–acridine agents cause permanent “covalent” damage in nucleolar rDNA because of their high level of accumulation in this subnuclear structure. We used ADAPT to enrich the Pt-damaged DNA isolated from cultured cancer cells and amplified the products by quantitative PCR (qPCR). To calculate the enrichment of APA-modified, biotinylated DNA relative to a sample of APA-modified, unbiotinylated DNA that was PCR-amplified using the same primers (negative control), we used the *percent of input* method<sup>[14]</sup> (see the Experimental Section). Primer pairs previously validated for rDNA analysis<sup>[15]</sup> were used to first pre-screen the 13.3-kb 47S pre-rRNA gene for Pt adducts within the coding (*coding*) region, the low-affinity Pol I-binding region (*gap*), and putative G-quadruplex forming sequences (*rg4*).<sup>[15]</sup> Adduct formation in the noncoding intergeneric spacer (*igs*) as well as the promoter and transcription regulating regions (*prom* and *ctcf*) was also assessed (Figure 4A).<sup>[15]</sup> For comparison, we also included primers for the housekeeping gene *GAPDH* and the oncogene *KRAS* (both located on chromosome 12), and for mitochondrial genomic DNA (mtDNA) (see the Experimental Section and Table S2 for sequence information).

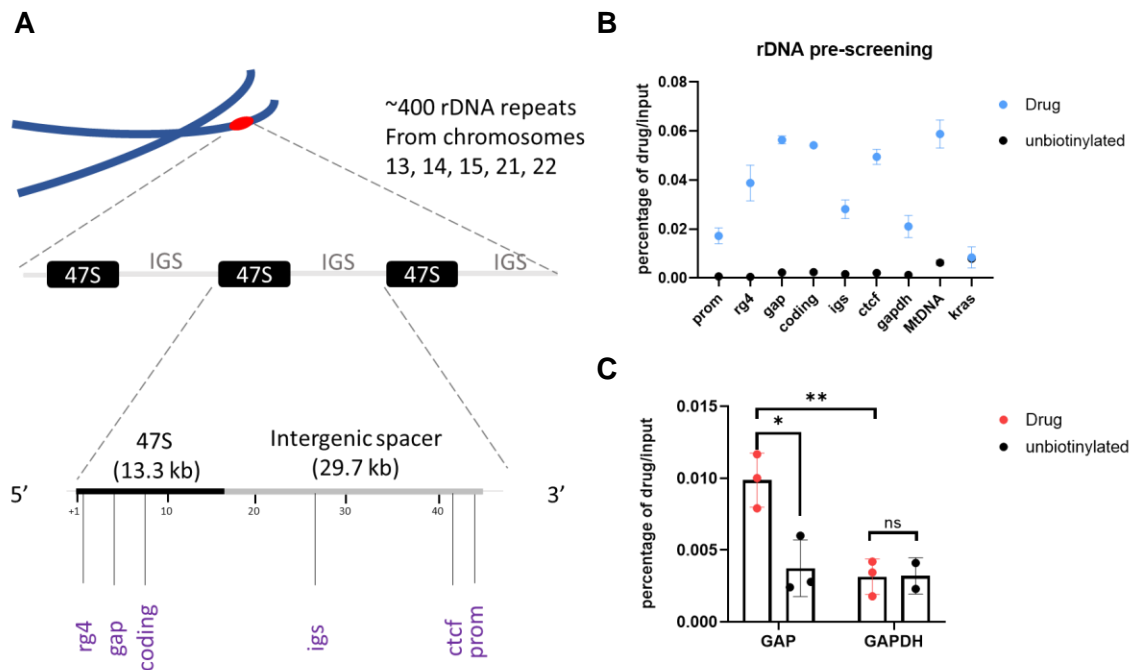


**Figure 4.** Application of ADAPT-qPCR to DNA extracted from APA-treated A549 lung cancer cells. (A) Map of human rDNA tandem repeats and locations of sequences screened in this study. (B) Pre-screening for adducts in rDNA, *GAPDH*, *mtDNA*, and *KRAS* sequences. Samples of drug-modified DNA ('drug') not subjected to the post-labeling step ('unbiotinylated') were included as negative control. qPCR results were calculated using percent of input method. (C) Comparison of target enrichment for two selected primer sets. Data shown are means of three biological independent experiments each performed with three technical replicates; mean  $\pm$  s.d.; \*\*,  $p < 0.01$  and \*,  $p < 0.05$ ; n.s., not significant,  $p > 0.05$ ; two-way ANOVA with Tukey post-hoc test. The higher relative enrichments observed for all primers compared to negative controls in (B) vs (C) are due to the larger number of amplification cycles employed, resulting in higher calculated drug/input values.

Details of the cell treatments and extraction of genomic DNA are presented in the Experimental Section. After reversal of the APA–DNA adducts, the purified genomic DNA was amplified with the appropriate primer pairs. Figure 4B shows the results of a pre-screening experiment in which three of the six rDNA primers – *gap*, *coding*, and *ctcf* – produced the highest amplification and enrichment levels. Significant enrichment ( $p < 0.05$ ) over non-post-labeled control groups was also observed for the primer set used to monitor APA-induced damage in mitochondrial DNA (mtDNA), but not for primers used to amplify the *GAPDH* and *KRAS* sequences. Based on these results, *gap*, which consistently showed the highest enrichment among all rDNA primers, was screened along with *GAPDH* in three additional, biologically independent experiments. The results confirm that *gap*-amplified DNA was significantly enriched over the negative control pulldown by approximately 2.6-fold and relative to *GAPDH*, for which enrichment proved to be not significant (Figure 4C). This outcome provides evidence that platinum–acridines induce permanent adducts in rDNA and that the G-rich (73% for 45S sequence; NCBI reference: NR 046235) pre-rRNA gene is a direct cellular target of platinum–acridines. The pronounced enrichment observed for mtDNA is surprising since accumulation of platinum–acridines in the cells' mitochondria has been firmly ruled out in co-staining/colocalization images captured by confocal microscopy.<sup>[3b, 10]</sup> It is possible that APA reacts with mitochondrial DNA that has been released into the cytoplasm (cytosolic mtDNA), as a consequence of genotoxic stress and during apoptotic signaling.<sup>[16]</sup>

Variations in sequence enrichment are not only observed between genes, but also within the same gene. It is known that factors such as transcriptional status and chromatin state affect the DNA binding efficiency of drugs and chemical probes.<sup>[17]</sup> Thus, the higher enrichment of sequences amplified with the primer sets *gap*, *coding*, and *ctcf* compared to other rDNA primers

may indicate a higher binding affinity of APA for these regions due to a more accessible nucleosome structure.<sup>[15]</sup> A large portion of the rDNA repeats, including actively transcribed and transcriptionally inactive sequences, exist in a loosely packaged, non-nucleosomal state,<sup>[18]</sup> and thus may be highly susceptible to the formation of monofunctional–intercalative adducts. Alternatively, the trends in enrichment may simply be caused by differences in APA–DNA adduct frequency in primer-specific amplicons, depending on G content. To evaluate this possibility, we quantified potential binding sites in the rDNA *gap* and *GAPDH* amplicons. A total of 20 putative high-affinity binding sites (base-pair steps) were identified within the amplified 103-bp rDNA sequence (19%) and 18 within the 95-bp fragment of *GAPDH* (19%), suggesting that the differences in enrichment are not related to nucleobase content and sequence context. Furthermore, the normalization method by which relative enrichment was calculated should rule out the possibility that differences in gene copy number (~400 for rDNA vs. 2 for *GAPDH*) may be responsible for the differences in PCR amplification yields.

The central role of the nucleolus in ribosome biogenesis, which fuels aggressive cancer growth,<sup>[8]</sup> and the fact that DNA double-strand break repair in the nucleolus is inefficient and error prone<sup>[19]</sup> may render it an ideal target for platinum–acridines. Consequently, the formation of cytotoxic PA–rDNA adducts and their downstream effects on ribosome biogenesis might help overcome drug resistance in DNA repair-proficient cancers.

## Conclusion

In summary, we have developed a chemical-biology tool to address an important mechanistic detail of a promising DNA-targeted agent at the cellular level. This was possible after turning the parent drug, PA, into an azide-functionalized chemical probe, APA. The method allows chemical pull-down of platinum-modified genomic DNA sequences extracted from cells by taking advantage of ex-vivo biotinylation via strain-promoted click chemistry. The qPCR-based enrichment pattern supports the hypothesis that rDNA is a direct target of platinum–acridines. ADAPT, in combination with next generation sequencing (“DNA-ADAPT-seq”), may provide an opportunity to generate a more comprehensive and unbiased map of the genomic targets of these hybrid agents.

## Experimental Section

### Materials and methods

The plasmids pUC19 (SD0061) and pBR322 (SD0041), restriction enzymes *EcoRI* (FD0274), *PstI* (FD0614), and *BamHI* (FD0054), DNase I enzyme (EN0521), and the 100-bp DNA ladder (15628-019) were purchased from Invitrogen/Thermo Fisher (Waltham, MA). Deoxyribonucleic acid sodium salt from calf thymus (D1501) was purchased from Sigma Aldrich (St. Louis, MO). DNA primers sequences (see Table S2) for qPCR amplifications were synthesized and purified by standard desalting by Eton Bioscience Inc. (Research Triangle Park, NC). Shrimp alkaline phosphatase (78390) was purchased from Affymetrix (Santa Clara, CA), and nuclease P1 (N7000) was purchased from USBiological (Salem, MA). DBCO-PEG<sub>4</sub>-BIOTIN (CAS. #1255942-07-4) was obtained from Click Chemistry Tools (Scottsdale, AZ). Dynabeads M-280 Streptavidin (11205D) and Dynabeads MyOne Streptavidin T1 (65601) were obtained from Invitrogen (Carlsbad, CA). Float-A-Lyzer G2 100–500 Da dialysis devices were from Spectra-Por (Sigma Aldrich, St. Louis, MO). All other biochemical grade reagents and synthetic precursors were purchased from common vendors and used as supplied. For additional supplies, see the description of specific assays.

<sup>1</sup>H NMR spectra of APA were recorded on a Bruker Ascend 400 MHz NMR instrument and are summarized in the conventional form including chemical shifts ( $\delta$ , ppm), multiplicities (s = singlet, d = doublet, t = triplet, q = quartet, m = multiplet, br = broad), coupling constants (Hz), and integral signal intensities. NMR spectra were processed and analyzed with MNova (version 12.0.3, Mestrelab Research, Escondido, CA). In-line LC-ES-MS analysis was performed on a Bruker AmaZon SL ion trap mass spectrometer equipped with an atmospheric pressure electrospray ionization (ESI) source and an in-line Shimadzu UFLC detector. Eluent nebulization

was achieved with a N<sub>2</sub> pressure of 44 psi, and solvent evaporation was assisted by a flow of N<sub>2</sub> drying gas (250 °C). Mass spectra were recorded in positive-ion mode with a capillary voltage of 4.5 kV over a mass-to-charge scan range of 150–2000 m/z. APA purity was determined in methanol containing 0.1% formic acid and separation of the diluted samples on a 4.6 mm × 150 mm reverse-phase Agilent ZORBAX SB-C18 (5 μm) analytical column at 25 °C using the following solvent system: solvent A, Optima water/ 0.1% formic acid, and solvent B, methanol/ 0.1% formic acid, at a flow rate of 0.4 mL/min and a gradient of 5% B for 5 min, 5% B–95% B over 15 min, 95% B for 10 min followed by 95% B–5% B over 5 min. Elution profiles were recorded at an acridine-specific wavelength at 413 nm. High resolution mass spectra for APA were obtained on a Thermo Orbitrap LTQ XL instrument equipped with Accela UPLC and autosampler. The spray voltage was 4 kV, and the temperature of the heated capillary was 300 °C. The sheath gas flow rate and the auxiliary gas flow rate were 31 and 13 (arbitrary units), respectively.

### Synthesis of [PtCl(pn)(C<sub>22</sub>H<sub>27</sub>N<sub>8</sub>O)](NO<sub>3</sub>)<sub>2</sub> (APA, dinitrate salt) (Scheme S1)

Compounds **1.2–1.9** were synthesized according to previously published procedures.<sup>[7a]</sup> The platinum–nitrile complex [PtCl(pn)(MeCN)]Cl (pn = propane-1,3-diamine) (**1.9**) (136 mg, 0.357 mmol) was converted to its nitrite salt via anion exchange with AgNO<sub>3</sub> (58 mg, 0.34 mmol) in 0.5 mL of anhydrous DMF. AgCl was removed by syringe filtration and the filtrate was cooled to -20 °C. The azide-modified acridine precursor **1.8** (135 mg, 0.357 mmol) was dissolved in 0.5 mL of anhydrous DMF and added to the filtrate, and the mixture was stirred at 4 °C for 24 hours before it was allowed to warm to room temperature. After treatment with activated carbon, the reaction mixture was precipitated in 300 mL of vigorously stirred diethyl ether. The product was collected

by membrane filtration and dried in a vacuum overnight. The crude mononitrate salt was re-dissolved in methanol containing one equivalent of aqueous 1 M HNO<sub>3</sub>, and the resulting dinitrate salt was recovered by precipitation with anhydrous diethyl ether. The product was further purified by recrystallization from hot ethanol to give 246 mg of APA as a yellow microcrystalline solid (Yield: 88%). <sup>1</sup>H NMR (400 MHz, DMF-d<sub>7</sub>) δ 13.89 (s, 1H), 9.88 (s, 1H), 8.70 (d, J = 8.7 Hz, 2H), 8.35 (t, J = 5.6 Hz, 1H), 8.12 – 7.94 (m, 3H), 7.65 (ddd, J = 8.3, 6.5, 1.4 Hz, 2H), 6.51 (s, 1H), 5.42 (s, 2H), 5.02 (s, 2H), 4.51 (s, 2H), 4.12 (t, J = 7.3 Hz, 3H), 3.83 (t, J = 6.7 Hz, 2H), 3.49 (s, 6H), 3.48 – 3.32 (m, 4H), 2.60 (t, J = 6.7 Hz, 2H), 1.82 (d, J = 6.6 Hz, 3H). Analytical purity (by LC-MS): 100%. HRMS (ESI, positive-ion mode): *m/z* for C<sub>25</sub>H<sub>36</sub>CIN<sub>10</sub>OPt ([M]<sup>+</sup>), calculated, 722.24043; found, 722.23944 (1.37 ppm). C<sub>25</sub>H<sub>37</sub>CIN<sub>10</sub>OPt ([M]<sup>2+</sup>), calculated, 362.12394; found, 362.12355 (1.08 ppm).

### General cell culture maintenance

The human cancer cell line A549 (lung adenocarcinoma, doubling time 21 h) was obtained from the American Type Culture Collection (ATCC) (Manassas, VA, USA) and cultured in DMEM/F12 media (Thermo Fisher, 11330-032) supplemented with 10% FBS (Thermo Fisher, A3160601) and 1% penicillin-streptomycin (Thermo Fisher, 15070-063). Cells were incubated at a constant temperature at 37 °C in a humidified atmosphere containing 5% CO<sub>2</sub> and subcultured every 2–3 days. The maximum passage number for A549 cells was 20, and cells were tested periodically for mycoplasma infections by fluorescence microscopy after staining with Hoechst 33258 dye.

### **Cell proliferation assay**

Cell proliferation assays were conducted using the CellTiter 96 kit as described previously.<sup>[4b]</sup> A549 cells were harvested and seeded in 96-well plates at a density of 5000 cells/well and allowed to attach overnight in the incubator prior to treatment with serially diluted APA for 72 hours. To assess cell viability, 20  $\mu$ L of a mixture of MTS/PMS solution was added to each well, and incubation was continued for 1–2 h. Conversion of MTS to formazan was quantified by absorbance measurements at 490 nm using a plate reader (Synergy HTX, BioTek, Winooski, VT). Cell viability was calculated as a percentage of untreated control. Three individual experiments were performed in triplicate wells. IC<sub>50</sub> values were calculated from nonlinear curve fits of the log[drug] vs. response data in GraphPad Prism (La Jolla, CA) and are reported as the mean  $\pm$  standard deviation (SD).

### **Quantification of APA–DNA adducts by inductively coupled plasma mass spectrometry (ICP-MS)**

700,000 A549 cells in 2.5 mL of complete DMEM/F12 media were seeded into T-25 flasks and allowed to attach overnight. Cells were then treated with 10  $\mu$ M APA for 6 h. Drug-containing medium was aspirated, and cells were washed 3  $\times$  with fresh media. Trypsin was added to detach cells, and 3 mL of fresh medium was added to each flask to collect the cell suspensions, which were pelleted by centrifugation at 250  $\times$  g for 5 min. After the supernatant was aspirated, pellets were washed with 2  $\times$  3 mL of PBS solution and centrifuged again at 250  $\times$  g for 3 min. Genomic DNA was extracted and purified using the AllPrep DNA/RNA Mini Kit (Thermo Fisher, 80204) following the manufacturer's protocol. The yield and purity of DNA harvested from each

experiment was determined using a Nanodrop™ 2000/2000c Spectrophotometer (average of two readings with 1  $\mu\text{L}$  per run). The extracted DNA had an  $A_{260}/A_{280}$  ratio of  $\sim 1.8$ . Pelleted cells were homogenized by microwave-assisted digestion (ETHOS UP Milestone, Sorisole, Italy) in trace-metal grade  $\text{HCl}/\text{HNO}_3$ . Standard curves were generated with appropriately diluted Pt standard (High-Purity Standards, Charleston, SC). Samples were analyzed on a 8800 Triple Quadrupole ICP-MS spectrometer (Agilent, Tokyo, Japan) equipped with a SPS 4 automatic sampler, a Scott-type double pass spray chamber operated at 2  $^\circ\text{C}$ , and a Micromist concentric nebulizer. Helium gas ( $\geq 99.999\%$ , Airgas, Colfax, NC) was used in the collision/reaction cell to minimize potential spectral interferences while monitoring the isotope  $^{195}\text{Pt}$ . The APA-to-DNA base pair ratio was calculated for triplicate experiments.

### **Enzymatic digestion and mass spectrometric analysis of platinum-modified DNA**

Calf thymus DNA was treated with APA at a drug-to-base pair ratio of 0.05 in 10 mM Tris buffer at 37  $^\circ\text{C}$  for 24 h. A fraction of the sample was removed and treated with 1 equivalent of DBCO-PEG<sub>4</sub>-BIOTIN at room temperature for an additional 24 h. Enzymatic digestions were performed with 100  $\mu\text{L}$  of the platinum-modified DNA samples using the following protocol (incubation times at 37  $^\circ\text{C}$ ): (i) 10  $\mu\text{L}$  50 mM  $\text{MnCl}_2$  + 10 u DNase I (2 h); (ii) 6.5 u of DNase I (2 h); (iii) 4 u nuclease P1 (2 h); (iv) 1 u nuclease P1 (16 h); (v) 10  $\mu\text{L}$  of 10  $\times$  alkaline phosphatase buffer (200 mM Tris-HCl, pH 8.0 and 100 mM  $\text{MgCl}_2$ ) + 5 u alkaline phosphatase; (vi) 3 u alkaline phosphatase. The mixtures were heat denatured at 65  $^\circ\text{C}$  for 15 min, centrifuged at 13000 rpm for 5 min, and the supernatants were collected. The digested samples were desalted against water overnight at 4  $^\circ\text{C}$  using Float-A-Lyzer disposable dialysis tubes (100-500 Da cut-off). Samples

were finally lyophilized and redissolved in 80  $\mu$ L of 0.1% formic acid in HPLC grade water for LC-MS analysis.

Sample analysis was performed on a Bruker Amazon-SL ion trap mass spectrometer equipped with an atmospheric pressure electrospray ionization (ESI) source and an in-line Shimadzu UFLC detector. Eluent nebulization was achieved with a N<sub>2</sub> pressure of 44 psi, and solvent evaporation was assisted by a flow of N<sub>2</sub> drying gas (250 °C). Mass spectra were recorded in positive-ion mode with a capillary voltage of 3 kV over a 150–2000 m/z scan range. Prior to MS/MS analysis of DNA fragments, precursor ions were identified in HPLC traces after separation of the diluted samples on a 4.6 mm  $\times$  150 mm reverse-phase Agilent ZORBAX SB-C18 (5  $\mu$ m) analytical column at 25 °C using the following solvent system: solvent A, optima water/0.1% formic acid, solvent B, acetonitrile/0.1% formic acid at a flow rate of 0.75 mL/min; 5% B to 27% B over 22 min, 27% B to 95% B from 22 min to 25 min; maintain at 95% B from 25 min to 32 min, and 95% B to 5% B from 32 min to 40 min. Elution of APA-modified and post-biotinylated APA-modified DNA fragments was monitored at 413 nm and in total ion count (TIC) chromatographs. Fragmentation of selected ions in MS/MS experiments was achieved by collision induced dissociation (CID) for target masses in Smart Parameter Setting (SPS) mode with an isolation width of 4.0. The Compass Data Analysis software suite (Bruker Daltonics, Billerica, MA) was used for peak integration.

### **DNA-ADAPT optimization in cell free systems**

pUC19 DNA (2686 bp) and pBR322 DNA (4361 bp) were linearized by treatment with *Eco*RI according to manufacturer's protocol. Then, 10  $\mu$ g of linearized pBR322 were treated with APA

at a drug-to-base pair ratio of 0.01 for 24 h at 37 °C in FastDigest buffer provided with the enzyme. After completion of the reaction, 10 µg of linearized pUC19 were added, and the sample was thoroughly mixed and supplemented with 1 equivalent (based on APA) of DBCO-PEG<sub>4</sub>-BIOTIN. This mixture was stored at room temperature for 24 h. M-280 dynabeads were added at a ratio of 1 mg of the beads per 10 µg of DNA, and samples were gently vertically mixed for 1 h using a Multi-Mix tube rotator (VWR). Beads were recovered from the mixtures using a Dyna-Mag-Spin magnet (Invitrogen) and washed 3 times with B&W buffer (5 mM Tris-HCl, 0.5 mM EDTA, 1 M NaCl, pH 7.5). To retrieve the affinity-captured DNA, the beads were resuspended in 100 µL of 3 mM aqueous NaCN solution and vertically mixed at 37 °C for 24 h. The supernatant was collected, lyophilized, and redissolved in Millipore water for downstream applications. Assays performed with pBR322 after digestion with *EcoRI*, *BamHI*, and *PstI*, and affinity capture of APA-modified DNA ladder were performed in the same manner. Samples were analyzed by electrophoresis on 1–1.5% agarose gels (70 V, room temperature, running time 2.5 h, TAE buffer, pH 8.3). Gels were pre-stained with ethidium bromide (1 µg/mL). Each lane contained approximately 100 ng of DNA. Gels were photo-documented using an Amersham Imager 600 (GE Healthcare), and band intensities were integrated with Image J (version 1.52a, National Institutes of Health, Bethesda, MD).

### **Isolation of APA-modified DNA from A549 lung cancer cells**

A549 cells at 90% confluency were harvested from three T-75 culture flasks, which had been subcultured at least three times. One day prior to treatment with APA,  $4 \times 10^6$  cells were plated in each of four 10-cm cell culture dishes in 8 mL of DMEM/F12 media (supplemented with

penstrep, and FBS) and allowed to attach overnight at 37 °C in a humidified atmosphere of 5% CO<sub>2</sub>. On the day of treatment, culture media was replaced with fresh media, and APA (10 mM stock solution in DMF) was added to afford a final drug concentration of 10 μM. Cells were then returned to the incubator for 6 h. The APA-containing media was removed from each dish, and the cells were washed twice with 2 mL of warm PBS. Cells were detached with 2 mL of warm trypsin-EDTA solution and transferred into 15-mL conical tubes after addition of 6 mL of medium to quench the trypsin. The cells suspensions were centrifuged for 5 min at 250 × g at 4 °C, and the supernatant was aspirated. Cell pellets can be flash-frozen in liquid nitrogen and stored at -80 °C for later analysis. Genomic DNA was extracted from the pellets and purified using the AllPrep DNA/RNA Mini Kit (Thermo Fisher, 80204) following the manufacturer's protocol. The yield and purity of DNA harvested from each experiment was determined using a Nanodrop™ 2000/2000c Spectrophotometer (average of two readings with 1 μL per run). The recovered DNA showed an A<sub>260</sub>/A<sub>280</sub> ratio of ~1.8.

### **Preparation of post-labeled genomic DNA for qPCR**

Genomic DNA samples were sheared at 4 °C for 5 min using a Sonicator Q800R (QSonica, Newtown, CT) ('15 sec on–15 sec off' cycles at 20% amplitude) to the desired fragment range of 100–1000 bp, which was confirmed by electrophoresis on 1.2% agarose gels. The DNA was then aliquoted at 10 μg in 100 μL of autoclaved water into sample tubes. Prior to post-labeling, 2 μL of each sample were removed and set aside as input control for qPCR amplification. The APA-modified genomic DNA samples were then either treated with DBCO-PEG<sub>4</sub>-BIOTIN to generate biotinylated DNA or left untreated to serve as unbiotinylated negative controls. The amount of

DBCO-PEG<sub>4</sub>-BIOTIN required to label all APA–DNA adducts in each sample was estimated from the adduct frequency determined by ICP-MS (drug-to-base pair ratio of 0.0005, equivalent to 0.775 pmol of label per  $\mu\text{g}$  of DNA). Accordingly, samples were treated with 1.1 equivalent of DBCO-PEG<sub>4</sub>-BIOTIN and incubated at room temperature for 16 h.

Prior to affinity purification, Dynabeads MyOne Streptavidin T1 (65601) were pre-washed for 5 min once with 1000  $\mu\text{L}$  of 1  $\times$  Binding and Washing (B&W)/Tween buffer and twice with 1000  $\mu\text{L}$  of 1  $\times$  B&W buffer. T1 beads were then resuspended in 2  $\times$  B&W buffer equivalent to twice the original suspended bead volume. [B&W buffer (2  $\times$ ) contained 10 mM Tris-HCl (pH 7.5) 1 mM EDTA, 2 M NaCl; B&W/Tween buffer (2  $\times$ ) contained 10 mM Tris-HCl (pH 7.5) 1 mM EDTA, 2 M NaCl, 0.1% Tween 20]. 50  $\mu\text{L}$  of the beads was added to 100 mL of the sheared DNA, and the mixture was incubated at room temperature for 30 min with continuous agitation by vertical rotation. The beads were washed three times for 7 min with 500  $\mu\text{L}$  of 1  $\times$  B&W/Tween buffer and twice with 500  $\mu\text{L}$  of 1  $\times$  B&W buffer. To reverse the Pt-DNA adducts and release the affinity-purified DNA from the beads, 100  $\mu\text{L}$  of 3 mM sodium cyanide solution was added to the mixture and incubation was continued for another 16 h at 37 °C. The same procedure was performed for each biotinylated and unbiotinylated sample. All DNA samples were finally purified using a Qiaquick PCR Purification Kit (28104) (Qiagen, Germantown, MD) prior to qPCR analysis.

### **Quantitative PCR**

Quantitative PCR (qPCR) was performed on a QuantStudio 3 Real-Time PCR System (ThermoFisher). PCR reaction mixtures (10  $\mu\text{L}$ ) contained SYBR Select Master Mix (Applied

Biosystems), 200 nM of each primer, diluted input, diluted template DNA, and autoclaved water depending on the specific experiment. Three technical replicates were run for each sample. PCR reactions consisted of one cycle at 50 °C for 2 min and 95 °C for 2 min, followed by 40 cycles at 95 °C for 15 s and 60 °C for 1 min, and a final melting curve analysis at 60 °C to 95 °C for 15 s, 95 °C to 60 °C for 1 min, and 95 °C for 1 s. The percent of input method<sup>[20]</sup> was used to calculate enrichments:

$$\text{Adjusted input} = \text{average } C_t - \log_2 50 \quad (1)$$

$$\% \text{ Input} = 100 \times 2^{(\text{adjusted input} - C_t)} \quad (2)$$

Statistical significance of experimental results for two-sample group comparisons was determined with a two-tailed Student t-test. One-way ANOVA with Tukey post-hoc test and 95% confidence intervals was used for comparisons of three or more sample groups with one independent variable (GraphPad Prism 8, GraphPad Software, San Diego, CA).

### *Acknowledgements*

This work was supported in part by NIH Cancer Center Grant P30 CA012197 and by Wake Forest Innovations. The authors thank Drs. Ke Zhang and Bahjat Fadi Marayati (WFU Department of Biology) for technical advice with the qPCR experiments.

### **Conflict of Interest**

The authors declare no conflict of interest.

**Keywords:** Antitumor agent · Click chemistry · DNA damage · Platinum · pre-rRNA gene

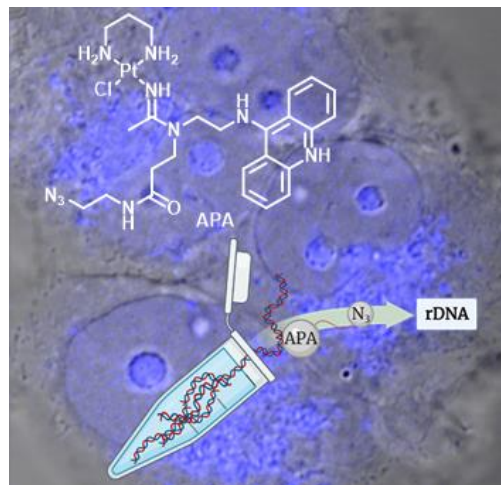
## References

- [1] a) S. Solier, S. Muller, R. Rodriguez, *Curr. Opin. Chem. Biol.* **2020**, *56*, 42-50; b) G. S. Erwin, D. Bhimsaria, A. Eguchi, A. Z. Ansari, *Angew. Chem. Int. Ed.* **2014**, *53*, 10124-10128; c) C. Jin, L. Yang, M. Xie, C. Lin, D. Merkurjev, J. C. Yang, B. Tanasa, S. Oh, J. Zhang, K. A. Ohgi, H. Zhou, W. Li, C. P. Evans, S. Ding, M. G. Rosenfeld, *Proc. Natl. Acad. Sci. USA* **2014**, *111*, 9235-9240.
- [2] a) E. C. Sutton, C. E. McDevitt, M. V. Yglesias, R. M. Cunningham, V. J. DeRose, *Inorg. Chim. Acta* **2019**, *498*; b) J. D. White, M. M. Haley, V. J. DeRose, *Acc. Chem. Res.* **2016**, *49*, 56-66; c) J. C. Hu, J. D. Lieb, A. Sancar, S. Adar, *Proc. Natl. Acad. Sci. USA* **2016**, *113*, 11507-11512; d) X. T. Shu, X. S. Xiong, J. H. Song, C. He, C. Q. Yi, *Angew. Chem. Int. Ed.* **2016**, *55*, 14244-14247; e) N. J. Farrer, D. M. Griffith, *Curr. Opin. Chem. Biol.* **2020**, *55*, 59-68.
- [3] a) X. Qiao, S. Ding, F. Liu, G. L. Kucera, U. Bierbach, *J. Biol. Inorg. Chem.* **2014**, *19*, 415-426; b) S. Ding, X. Qiao, J. Suryadi, G. S. Marrs, G. L. Kucera, U. Bierbach, *Angew. Chem. Int. Ed.* **2013**, *52*, 3350-3354.
- [4] a) S. Zhang, X. Yao, N. H. Watkins, P. K. Rose, S. R. Caruso, C. S. Day, U. Bierbach, *Angew. Chem. Int. Ed.* **2020**, *59*, 21965-21970; b) X. Yao, N. H. Watkins, H. Brown-Harding, U. Bierbach, *Sci. Rep.* **2020**, *10*, 15201.

- [5] a) F. Liu, J. Suryadi, U. Bierbach, *Chem. Res. Toxicol.* **2015**, *28*, 2170-2178; b) X. Qiao, A. E. Zeitany, M. W. Wright, A. S. Essader, K. E. Levine, G. L. Kucera, U. Bierbach, *Metallomics* **2012**, 645-652; c) C. L. Smyre, G. Saluta, T. E. Kute, G. L. Kucera, U. Bierbach, *ACS Med. Chem. Lett.* **2011**, *2*, 870-874.
- [6] H. Kostrhunova, J. Malina, A. J. Pickard, J. Stepankova, M. Vojtiskova, J. Kasparikova, T. Muchova, M. L. Rohlfing, U. Bierbach, V. Brabec, *Mol. Pharmaceutics* **2011**, *8*, 1941-1954.
- [7] a) S. Ding, X. Qiao, G. L. Kucera, U. Bierbach, *J. Med. Chem.* **2012**, *55*, 10198-10203; b) K. Cheung-Ong, K. T. Song, Z. Ma, D. Shabtai, A. Y. Lee, D. Gallo, L. E. Heisler, G. W. Brown, U. Bierbach, G. Giaever, C. Nislow, *ACS Chem. Biol.* **2012**, *7*, 1892-1901; c) Z. Ma, L. Rao, U. Bierbach, *J. Med. Chem.* **2009**, *52*, 3424-3427.
- [8] J. Pelletier, G. Thomas, S. Volarevic, *Nat. Rev. Cancer* **2018**, *18*, 51-63.
- [9] M. van Sluis, B. McStay, *Curr. Opin. Cell Biol.* **2017**, *46*, 81-86.
- [10] A. J. Pickard, F. Liu, T. F. Bartenstein, L. G. Haines, K. E. Levine, G. L. Kucera, U. Bierbach, *Chem. Eur. J.* **2014**, *20*, 16174-16187.
- [11] J. R. Choudhury, L. Rao, U. Bierbach, *J. Biol. Inorg. Chem.* **2011**, *16*, 373-380.
- [12] R. Rodriguez, K. M. Miller, *Nat. Rev. Genet.* **2014**, *15*, 783-796.
- [13] H. L. Tytgat, G. Schoofs, M. Driesen, P. Proost, E. J. Van Damme, J. Vanderleyden, S. Lebeer, *Microb. Biotechnol.* **2015**, *8*, 164-168.
- [14] X. Lin, L. Tirichine, C. Bowler, *Plant Methods* **2012**, *8*, 48.
- [15] G. E. Zentner, A. Saiakhova, P. Manaenkov, M. D. Adams, P. C. Scacheri, *Nucleic Acids Res.* **2011**, *39*, 4949-4960.

- [16] J. S. Riley, G. Quarato, C. Cloix, J. Lopez, J. O'Prey, M. Pearson, J. Chapman, H. Sesaki, L. M. Carlin, J. F. Passos, A. P. Wheeler, A. Oberst, K. M. Ryan, S. W. Tait, *EMBO J.* **2018**, *37*, e99238.
- [17] a) J. Hu, J. D. Lieb, A. Sancar, S. Adar, *Proc. Natl. Acad. Sci. USA* **2016**, *113*, 11507-11512; b) X. Shu, X. Xiong, J. Song, C. He, C. Yi, *Angew. Chem. Int. Ed.* **2016**, *55*, 14246-14249.
- [18] M. Derenzini, G. Pasquinelli, M. F. O'Donohue, D. Ploton, M. Thiry, *J. Histochem. Cytochem.* **2006**, *54*, 131-145.
- [19] D. O. Warmerdam, R. M. F. Wolthuis, *Chromosome Res.* **2019**, *27*, 57-72.
- [20] M. Haring, S. Offermann, T. Danker, I. Horst, C. Peterhansel, M. Stam, *Plant Methods* **2007**, *3*, 1-16.

## TOC



The DNA damage caused by a platinum–acridine agent in cancer cells was studied using an assay that combined post-labeling of click chemistry-enabled DNA adducts, affinity pull-down purification, and PCR amplification. The method demonstrates that rDNA repeats are a cellular, and potentially pharmacological, target of the hybrid agents.